SIMULATION OF ECU IN PROTEUS FOR DIRECT INJECTION CONTROLLING FLEXIBLE SYNGAS-BIOGAS-HYDROGEN BLEND IN DUAL FUEL ENGINE

Nguyen Huu Hieu[1], Bui Van Hung[2], Ho Tran Ngoc Anh[2]*, Nguyen Minh Tien[2]

[1]*The University of Danang - University of Science and Technology, Vietnam*
[2]*The University of Danang - University of Technology and Education, Vietnam*

*Corresponding author: htnanh@ute.udn.vn

(Received: May 11, 2025; Revised: June 15, 2025; Accepted: June 20, 2025)

DOI: 10.31130/ud-jst.2025.23(9B).514E

Abstract - Direct injection through a twining injector system enables an increase in output power of dual-fuel engines, improves speed control capacity, and allows the engine to use flexible gaseous fuel blends of syngas-biogas-hydrogen with large variation of compositions. When the injection pressure is reduced from 5 bar to 3 bar, the start injection angle is advanced by 20°CA and the gauge pressure in the cylinder drops by 0.1 bar. In syngas fueling mode, with an injection pressure of 3.5 bar, to achieve ϕ=0.75 at a crankshaft position of 250°CA, the start injection angles are 80°CA, 50°CA, and 25°CA corresponding to engine speeds of 2000 rpm, 2400 rpm, and 2800 rpm, respectively. The gauge pressure in the cylinder increases by 100%, 97%, and 79%, respectively, compared to natural aspiration fueling mode.

Key words - Dual fuel engine; Direct injection gaseous fuels; Syngas; Biogas; Hydrogen.

1. Introduction

At the recent COP26 Climate Change Summit held in Glasgow, Vietnam committed to implementing mechanisms under the Paris Agreement to achieve net-zero emissions by 2050 [1]. To accomplish this goal, the Vietnamese government has undertaken an energy transition strategy, gradually replacing fossil fuels with renewable energy sources.

Although technologies for the production and use of renewable energy have significantly improved, their fundamental limitations have yet to be fully addressed by conventional solutions. In general, renewable energy sources are inherently unstable; the power output varies over time or changes randomly depending on climatic and weather conditions. Therefore, to ensure the stability of the energy system, it is necessary to integrate multiple renewable energy sources - forming what is known as a hybrid renewable energy system - rather than relying on a single, independent source [2]. Like many tropical countries, Vietnam has abundant potential for solar, wind, and biomass energy. Consequently, a hybrid renewable energy system combining syngas, biogas, solar, and wind energy - referred to as the SBS (Syngas-Biogas-Solar) renewable energy system - offers significant advantages [3–6].

In addition to the benefits of clean energy production, the SBS system also contributes to the treatment of solid waste from rural residential and agricultural activities. Non-biodegradable solid waste is processed into refuse-derived fuel (RDF) pellets, which are then gasified into syngas [8]. Biodegradable organic waste is used for biogas production. When the output of solar and wind energy exceeds the demand load, the surplus power is used to produce hydrogen. Syngas, biogas, and hydrogen are stored together in gas storage bags to supply fuel for electricity-generating engines when solar power is intermittent or insufficient to meet the load [7].

According to the operating principle of the aforementioned SBS renewable energy system, the composition of the gaseous fuel supplied to the engine varies randomly and across a wide range. The engine may operate entirely on a single fuel component or on a mixture of two or three fuel components in varying proportions [9–10]. A significant challenge for the intake system arises from the large disparity in air-fuel ratio (A/F) between syngas and the other fuels. Syngas has a notably lower A/F ratio, leading to prolonged injection durations, which in turn results in incomplete intake of the fuel into the cylinder by the end of the intake stroke. Consequently, the engine's equivalence ratio often cannot reach the stoichiometric value - especially at high engine speeds - thereby affecting combustion efficiency. Fuel accumulation in the intake port from previous cycles causes fluctuations in the equivalence ratio in subsequent cycles and can lead to backfire phenomena. The technique of enriching biogas with hydrogen for use in spark ignition engines has been studied in several works [11–12]. Research findings indicate that the most effective method for delivering hydrogen-enriched biogas is electronically controlled injection [13–18]. However, these strategies are no longer suitable when syngas is used as fuel. The significantly lower A/F ratio of syngas compared to conventional fuels presents a major technical challenge for fuel delivery systems. A proposed solution for engines running on flexible gaseous fuels is the implementation of a dual injection system [23, 24].

Another difficulty associated with syngas use is its low heating value, which leads to a reduction in engine power output. When air is used as the oxidizer, the volumetric composition of typical syngas includes approximately 18–20% H_2, 18–20% CO, 2% CH_4, 11–13% CO_2, traces of H_2O, and the remainder N_2 [21]. The typical lower heating value (LHV) of syngas ranges from 4 to 6 MJ/kg [19], which is only about 10% of the LHV of natural gas, LPG, or gasoline. However, because the required air mass for complete combustion of a unit mass of syngas is also roughly 10% of that for conventional fuels, the reduction in engine power is not directly proportional to its LHV. In

practice, engine power output is reduced by approximately 15–20% compared to diesel engines, and by 30–40% compared to gasoline engines when fueled with syngas [22]. A common approach to improve the performance of syngas-fueled engines is enriching the fuel with higher-heating value components such as biogas or hydrogen [20]. However, as described above, in hybrid renewable energy systems, the engine is supplied with a flexible fuel mixture of syngas, biogas, and hydrogen, whose composition can vary widely. Therefore, enriching syngas with biogas or hydrogen alone does not guarantee stable engine performance under fluctuating fuel supply conditions. A viable solution to this issue is direct injection of gaseous fuel into the engine cylinder, which improves the volumetric efficiency.

Currently, several engines use direct injection systems for conventional gaseous fuels such as LPG, CNG, and hydrogen. However, studies on direct-injection engines fueled with variable-composition renewable gas mixtures are extremely limited - particularly for dual-fuel engines operating on flexible syngas-biogas-hydrogen mixtures. In such engines, in addition to addressing fuel delivery challenges, the distribution of the fuel-air mixture within the combustion chamber must be carefully managed to ensure that the pilot injection has sufficient oxygen to enable auto-ignition.

In this study, we present simulation results of direct injection of gaseous fuel into the cylinder of a dual-fuel engine operating on a syngas-biogas-hydrogen mixture with flexible composition.

2. Research Methods and Equipment

2.1. Engine and Fuel

The research was conducted on a Vikyno RV165 engine with a cylinder diameter of 105mm, piston stroke of 97mm, and compression ratio of 20. When running on diesel, the engine produces a maximum power of 16.5 HP at a speed of 2400 rpm. When converted to a dual fuel engine using flexible syngas-biogas-hydrogen fuel, the engine combustion chamber was modified to reduce the compression ratio to 16.5.

Biogas, syngas, and hydrogen have the main characteristics presented in Table 1.

Table 1. *Characteristic parameters of the fuel*

Fuel	Composition (mol/mol)					M (g/mol)	m_{kk}/m_{nl} (g/g)	V_{kk}/V_{nl} (l/l)
	CH_4	H_2	CO	CO_2	N_2			
Biogas	0.7	0	0	0.3	0	24.40	7.98	6.71
Syngas	0.05	0.18	0.20	0.12	0.45	24.64	1.64	1.39
Hydrogen	0	1	0	0	0	2	34.78	2.4
Low heating value (MJ/m^3)	33.9	10.24	12.03	-	-			

2.2. Model setup

Simulation calculations were performed using Ansys Fluent 2021R1 software. The computational domain includes the combustion chamber and engine cylinder with volume varying according to crankshaft rotation angle. The engine combustion chamber has an omega shape. Gaseous fuel is directly injected into the engine cylinder through two injectors with a diameter of 6mm. The injector axes are located on the xy longitudinal cross-section of the cylinder, while the intake valve axis is located on the yz longitudinal cross-section of the cylinder.

The convection-diffusion equation system is closed using the k-epsilon turbulence model. Each time the fuel is changed, we recalculate the thermodynamic parameter pdf table. This allows the calculation boundary conditions to be simplified. At the intake inlet, there is only air, so the mixture fraction (f) equals 0. At the injector inlets, there is only fuel, so f=1. The local equivalence ratio of the mixture is calculated through the fuel and oxygen components or through f.

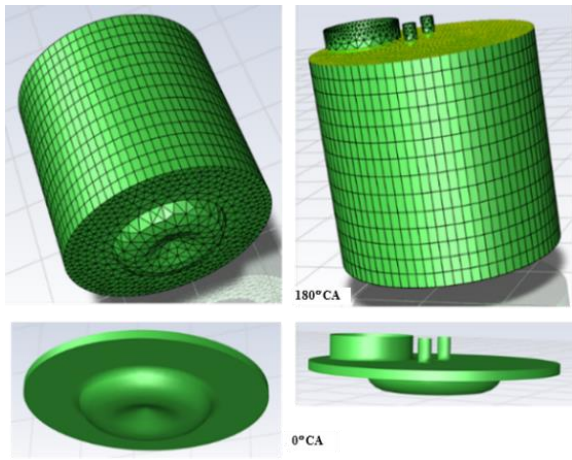

Figure 1. *Grid generation for the simulation domain*

Figure 1 introduces the combustion chamber, cylinder, intake port, injectors, and the computational mesh. The fuels used in the simulation are syngas, biogas, hydrogen, and mixtures of these. The engine runs at speeds of 2000 rpm, 2400 rpm, and 2800 rpm. The fuel injection pressure varies in the range from 3 bar to 5 bar.

3. Results and discussion

3.1. Injector Configuration and Injection Pressure

Figures 2a and 2b illustrate the variation in fuel concentration and velocity field within the cylinder on the xy and yz cross-sections at a piston position of 155°CA, when syngas is directly injected into the combustion chamber through a single injector and through two injectors, respectively. The engine operates at a speed of 2400 rpm, with injectors of 6 mm diameter and an injection pressure of 5 bar. In the single-injector configuration, when the fuel jet strikes the piston crown, part of the fuel reflects back, creating a recirculation zone toward the side of the combustion chamber opposite the intake valve. In contrast, the two-injector configuration generates a symmetric vortex structure about the cylinder centerline. In both cases, lean mixture regions are concentrated near the intake valve. At the same piston position (155°CA), the lean mixture region is narrower with the two-injector setup compared to the single-injector case. Under identical injection pressure and start-of-injection timing, the peak fuel concentration in the cylinder with two injectors is

nearly twice that of the single-injector configuration. Consequently, to achieve the same mixture equivalence ratio, the injection duration must be longer in the single-injector case. This extended injection period leads to increased compression pressure within the combustion chamber, thereby raising the engine's pumping loss. Moreover, a longer injection duration under rising in-cylinder pressure results in backpressure effects that reduce the actual injection mass flow rate.

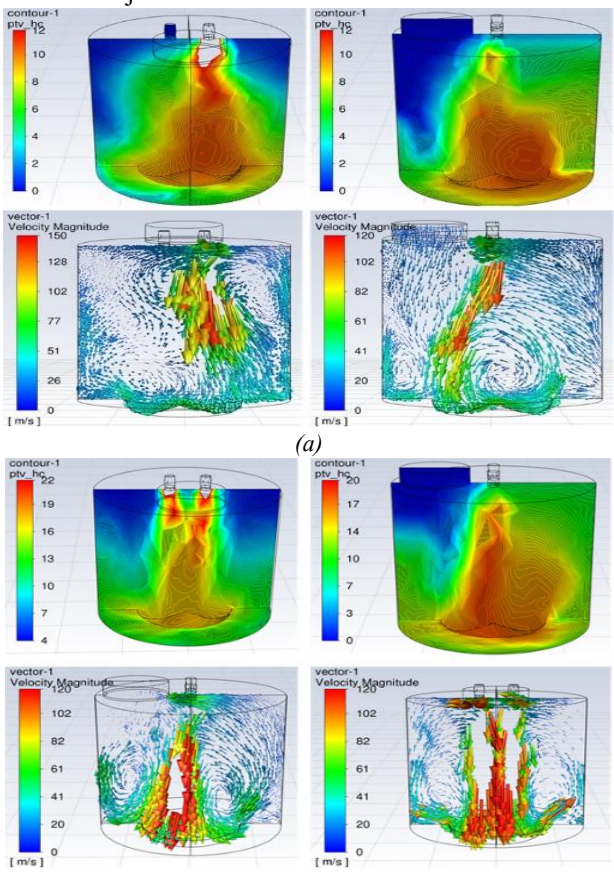

Figure 2. *Variation of fuel concentration and velocity field in the cylinder on the xy and yz cross-sections during direct injection of syngas through (a) single injector and (b) dual injector at a piston position of 155°CA, (p_p= 5 bar, φ_{start}=30° CA)*

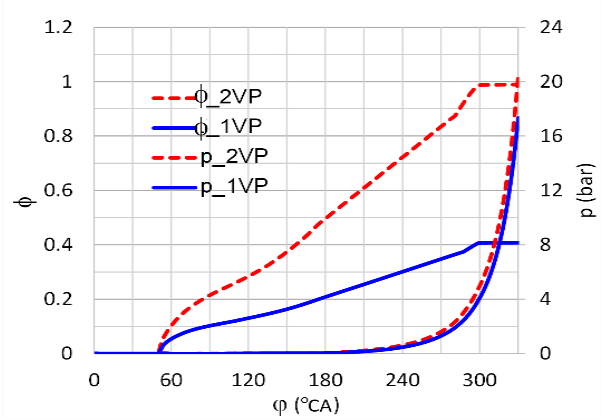

Figure 3. *Variation of equivalence ratio and in-cylinder pressure with crank angle for syngas injection using one injector and two injectors (n=2400 rpm, φ_{start}=50°CA)*

Figure 3 shows the variation of the equivalence ratio and in-cylinder pressure in the cases of syngas injection through one injector and two injectors. In both cases, the injectors start to open at φ_{start} = 50° crank angle (CA) with an injection pressure of 5 bar. At 180° CA, the equivalence ratio in the one-injector case reaches φ = 0.21, while in the two-injector case it reaches φ = 0.5. At 240° CA, the equivalence ratios are 0.3 and 0.71, respectively. By 300° CA, near the end of the compression stroke, the equivalence ratio with one injector only reaches 0.4. This indicates that with a single 6 mm injector operating at 5 bar, the mixture cannot reach φ = 1 even if injection starts right at the beginning of the intake stroke. In contrast, with two injectors, there is a sufficiently large crank angle window to adjust the mixture composition when engine speed or load conditions change.

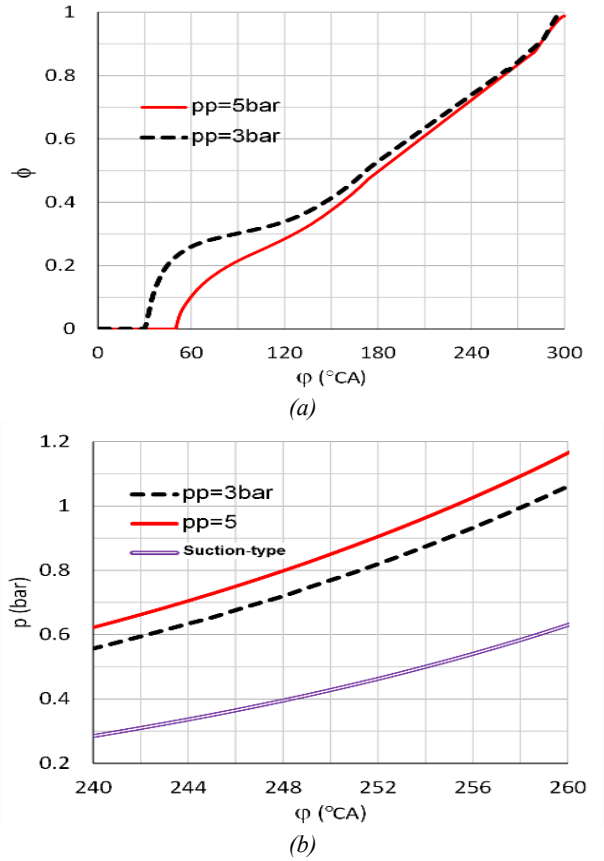

Figure 4. *Effect of injection pressure on the variation of (a) equivalence ratio and (b) in-cylinder pressure with crank angle (engine speed n = 2400 rpm, dual injector)*

Similar to the case of spark-ignition engines using syngas, when using single injector, the flow diameter must be sufficiently large or the injection pressure must be elevated [23, 24]. This introduces challenges for the fuel compression system prior to delivery to the engine, as well as for injector sealing techniques, particularly for direct injectors integrated into the engine's combustion chamber. Furthermore, for the engine to be capable of utilizing multiple types of renewable gaseous fuels, the fuel supply system must possess the adaptability to accommodate variations in fuel composition.

When the injection pressure is reduced, the injection

timing must be advanced to ensure that the equivalence ratio is maintained by the conclusion of the injection process. Figure 4a compares the variation of the equivalence ratio with crank angle when the injection pressure is set to 5 bar and 3 bar, respectively, at an engine speed of 2400 rpm. In the case of 3 bar injection pressure, the injection start occurs at 30°CA, while at 5 bar, injection starts at 50°CA. In both cases, at the piston position of 250°CA, the equivalence ratio of the mixture reaches 0.75. Figure 4a illustrates that as the injection pressure decreases from 5 bar to 3 bar, the equivalence ratio of syngas shifts between 0.6 and 0.9, requiring the injector to open 20° earlier. At 5 bar injection pressure, the gas mixture pressure within the cylinder is, on average, 0.1 bar higher compared to the 3 bar injection pressure scenario. Consequently, the indicated mean effective pressure for the 3 bar injection case is lower than that for the 5 bar injection case.

During operation, the engine load is adjusted to ensure that the engine speed remains constant. When the engine load is reduced, the injection process ends earlier. This results in a decrease in the amount of injected fuel gas and, on the other hand, reduces the end-of-compression pressure (lowering the intake efficiency), which causes the engine load to drop more rapidly compared to a suction-type fuel supply. Conversely, when the load is increased, the process reverses. As a result, the torque curve of the syngas-injected engine is steeper than that of the suction-type engine, which facilitates the speed control process.

3.2. Formation of Syngas-Diesel Mixture

When using the direct injection solution, fuel can continue to be injected into the cylinder after the intake valve has closed. Figure 7a illustrates the fuel concentration distribution and the airflow velocity field inside the cylinder at the 240°CA position. In the early stage of the compression process, the fuel concentration is almost symmetrically distributed at the bottom of the cylinder, as the kinetic energy of the fuel spray is sufficient to control the motion of the surrounding air. However, at the top of the cylinder, the fuel concentration is low on the side of the cylinder containing the intake valve. At 330°CA, just before the start of the ignition spray, the fuel-rich mixture at the bottom of the combustion chamber is pushed upwards towards the top, moving towards the center of the combustion chamber. Although the airflow exhibits strong swirling motion, the side of the combustion chamber near the intake valve still continues to contain a fuel-lean mixture compared to the other half of the chamber (Figure 7b). This is a noteworthy difference between the direct injection syngas solution and the suction-type solution. At the end of the compression process, a small amount of diesel fuel is injected into the combustion chamber to ignite the syngas-air mixture. The diesel injection is typically about 10% to 15% of the full-load injection when the engine is running entirely on diesel. Figure 8 shows the pressure variation inside the cylinder, the diesel concentration, and the average equivalence ratio of the mixture as a function of crank angle. The engine runs at a speed of 2400 rpm, with an injection pressure of 5 bar, and the syngas injector opens at 50°CA and closes at 250°CA. Under these syngas injection conditions, the equivalence ratio of the syngas-generated mixture is 0.75. Diesel is injected into the combustion chamber at 340°CA and the injection ends at 350°CA. It is observed that when diesel is injected, its concentration increases, leading to an increase in the average equivalence ratio of the mixture to ϕ=0.9. Therefore, the contribution of diesel to the equivalence ratio is 0.15. Unlike the case of syngas injection, since diesel is a liquid fuel and the air/fuel ratio is much higher than that of syngas, its injection into the cylinder does not significantly alter the gas mixture pressure.

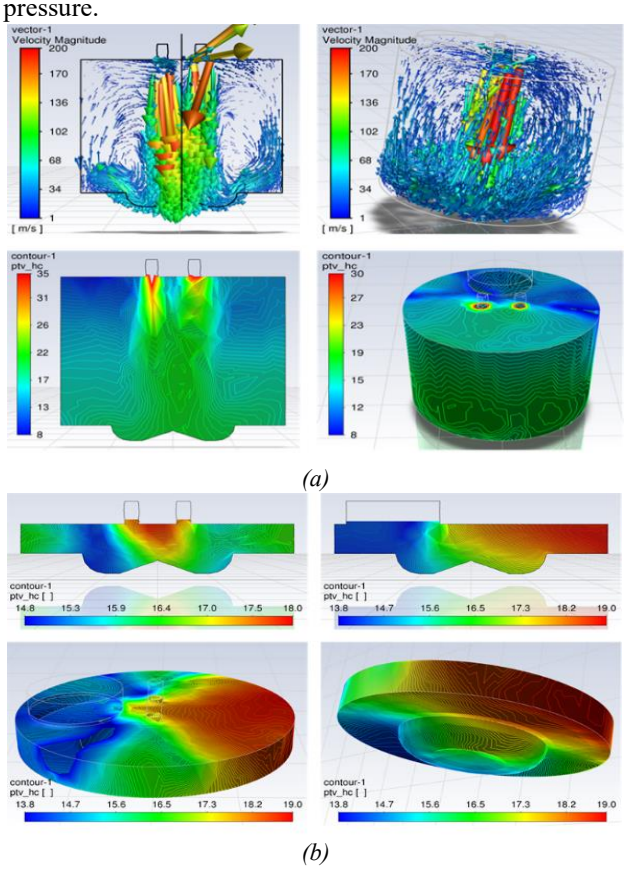

Figure 7. *Fuel concentration distribution inside the cylinder at the 240° CA position (p_p=5bar, φ_{start}=30°CA)*

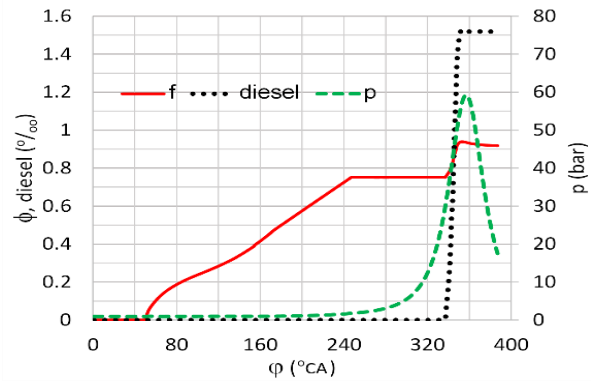

Figure 8. *Variation of in-cylinder pressure, diesel concentration, and equivalence ratio as a function of crank angle (n=2400 rpm, p_p=5 bar, syngas injector opens at 50°CA and closes at 250°CA, diesel injector opens at 340°CA and closes at 350°CA)*

Figure 9 illustrates that when diesel fuel is injected into the hot air mass inside the combustion chamber, it evaporates almost immediately. The evaporation curve increases sharply from the start of injection (at 340°CA) to the end of injection (at 350°CA). The fuel is almost completely evaporated at 360°CA when the engine runs at 2000 rpm, and at approximately 365°CA at 2800 rpm. As engine speed increases, the evaporation process takes longer in terms of crank angle due to the reduced time per crank degree. Under the same injection conditions, increasing engine speed results in a lower quantity of diesel injected into the combustion chamber, corresponding to a reduction in the equivalence ratio. At an injection pressure of 5 bar and an injection duration of 10°CA, the equivalence ratio contribution from diesel fuel is 0.15 at 2000 rpm, but only 0.1 at 2800 rpm. Therefore, the amount of diesel pilot injection must be adjusted according to the engine's operating speed to ensure a minimum quantity sufficient for reliable ignition of the mixture and for lubricating the injector.

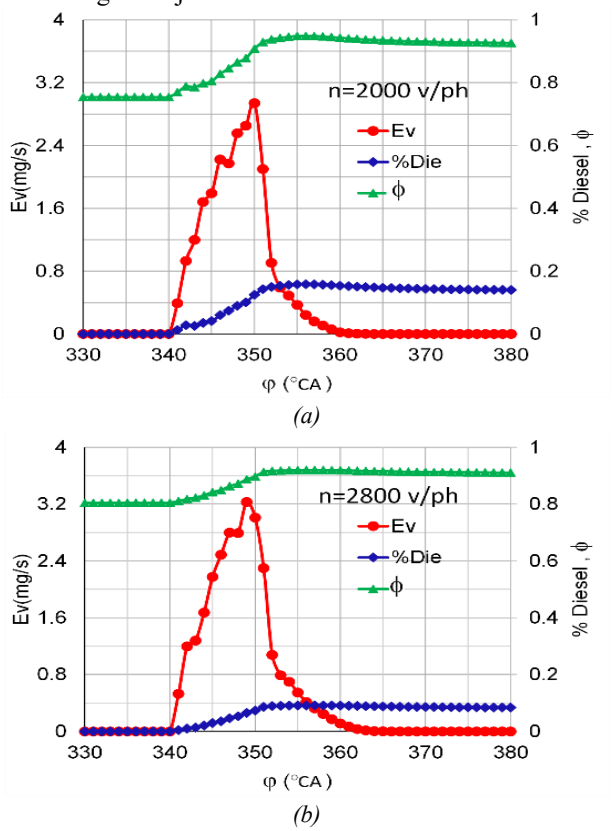

Figure 9. *Comparison of the variation in liquid fuel evaporation rate, diesel concentration, and equivalence ratio at engine speeds of 2000 rpm (a) and 2800 rpm (b)*

Figure 10 compares the distribution of fuel concentration and gas velocity in the cylinder at 380°CA for engine speeds of 2000 rpm and 2800 rpm, with the same equivalence ratio contribution from diesel injection set at 0.15. It can be observed that as engine speed increases, the variation in fuel concentration within the combustion chamber decreases. Specifically, as shown in Figure 10, the difference between the minimum and maximum fuel concentrations is 13%–20% at 2000 rpm, while at 2800 rpm, this range narrows slightly to 14%–19%.

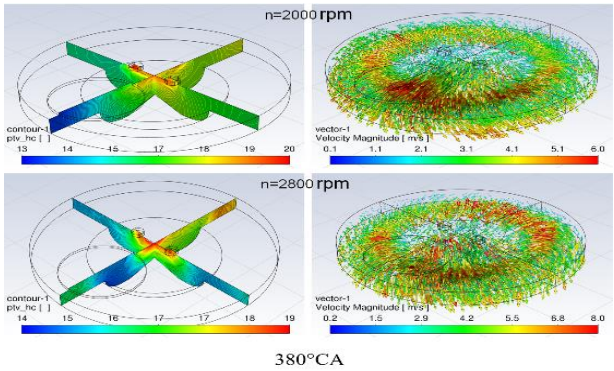

Figure 10. *Comparison of the fuel concentration field and velocity field at 380°CA for engine speeds of 2000 rpm and 2800 rpm*

3.3. Simulation of the injector control ECU in Proteus

The flexible direct injection system for syngas–biogas–hydrogen fuel in a dual-fuel engine is governed by a specially designed Electronic Control Unit (ECU). Prior to physical implementation, the ECU was simulated using Proteus software. Figure 11 illustrates the main components of the simulated ECU. The ECU is based on an Arduino Mega microcontroller. The engine load is represented by an electrical load, with voltage and current simulated via variable resistors labeled VOLT and AMP, respectively. Engine speed is emulated through the RPM variable resistor. Main operating parameters of the engine - including load, speed, and injection timing - are displayed on an LCD screen, while data are monitored via the serial monitor and recorded for analysis.

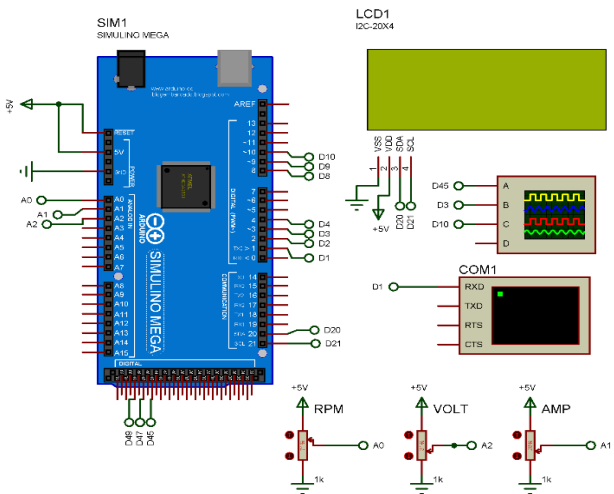

Figure 11. *Schematic of the Direct Injector Control ECU in Proteus*

The top dead center (TDC) and the injector control pulse are displayed on the virtual oscilloscope in Proteus.

The injector control software is installed on the Arduino microcontroller. The microcontroller receives input data including engine load and speed, calculates the appropriate injection duration, and generates the control signal for the injector. Figure 12 presents the simulation result of an ECU operation in Proteus for a case where the engine speed is 2987 RPM and the electrical load power is 3.519 kW. In this case, the injection duration is calculated to be 7.038 milliseconds.

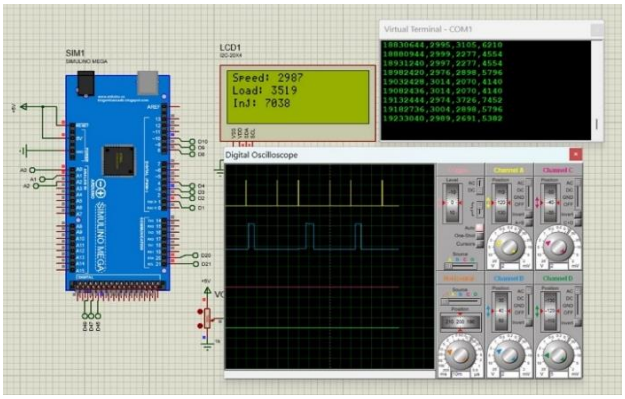

Figure 12. *Simulation results of the ECU operation in Proteus*

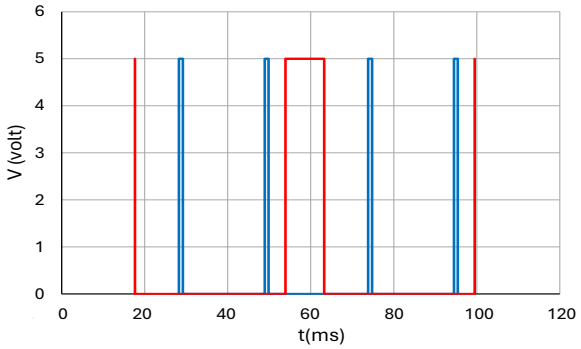

(a)

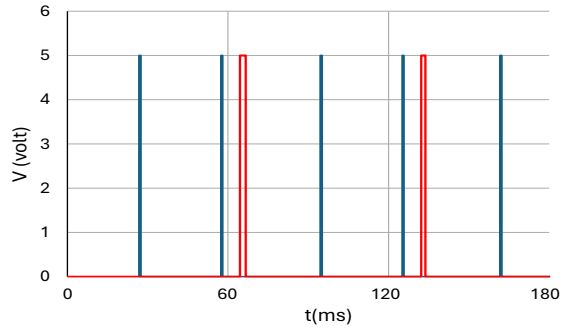

(b)

Figure 13. *TDC and injector control signal at engine speeds of 3000 RPM and 1000 RPM*

Figures 13a and 13b illustrate the TDC signal and the injector control signal when the engine operates at 3000 RPM and 1000 RPM, respectively. As the engine under study is a four-stroke engine, each cycle includes two TDC pulses with unequal spacing. The intake-compression duration lasts longer than the expansion-exhaust duration. This allows programming the injector control signal to activate only during the intake stroke, ensuring no injection occurs during the expansion stroke.

3.4. Retrofitting a diesel engine into a dual-fuel engine with direct injection of a syngas–biogas–hydrogen fuel mixture

After simulating the ECU and calibrating the control program in Proteus, a physical ECU was fabricated to control the direct gas injector. The direct gas injector was designed with a reverse-mounted nozzle compared to conventional intake-mounted injectors to avoid the influence of increased in-cylinder pressure during combustion. Figures 14a and 14b illustrate the technical drawing of the injector and its installation into the cylinder head of the dual-fuel engine. The injector was mounted onto a sleeve that was rigidly welded into the cylinder head. To prevent coolant leakage into the combustion chamber, the sleeve was welded both on the inner and outer surfaces.

The TDC sensor is a Hall-effect sensor mounted on a fixed bracket, with the sensor facing the toothed wheel. The number of teeth and the gear ratio from the engine crankshaft to the toothed wheel are designed such that one pulse is generated for each revolution of the engine. Furthermore, to optimize the fuel–air mixture, a lambda sensor is installed in the engine's exhaust manifold to measure the oxygen content in the exhaust gases.

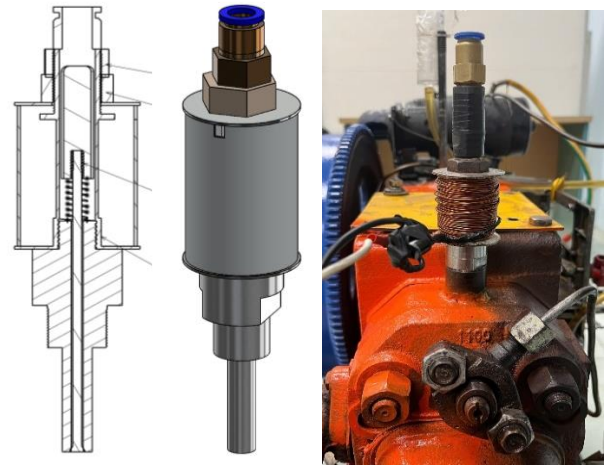

Figure 14. *Design of the direct injection nozzle (a) and installation of the nozzle into the cylinder head of the dual-fuel engine (b)*

Figure 15. *Arrangement of the TDC sensor (a) and the lambda sensor (b)*

Figure 16 illustrates the overall layout of the dual fuel engine experimental system. The system consists of a dual fuel engine running on a syngas-biogas-hydrogen mixture, with direct fuel injection via injectors and an ECU controlled by the results of the simulation study. The engine drives a 5 KW generator. The load consists of 10 halogen lamps, each with a power rating of 500 W. Initial test results indicate that the ECU operates well, providing a flexible syngas-biogas-hydrogen fuel mixture, with the engine running smoothly at different load and speed modes.

Figure 16. *Layout of the dual fuel engine using flexible syngas-biogas-hydrogen fuel in the experimental system*

4. Conclusion

The research results lead to the following key conclusions:

- Direct fuel injection is an effective solution to overcome the power loss typically encountered in engines operating with lean gaseous fuels. Due to the much lower air-to-fuel ratio of syngas compared to conventional fuels, flexible engines using renewable gaseous fuels should adopt dual injectors with adjustable opening and closing angles depending on fuel composition, load condition, and engine speed.

- To maintain stable peak power in direct-injection dual-fuel engines running on gaseous fuels, the fuel quantity supplied is controlled by adjusting the injection start timing. This injection timing is initially set based on the engine's maximum power and rated speed.

- When reducing injection pressure from 5 bar to 3 bar, the injection start angle needs to be advanced by 20°CA, and the in-cylinder residual pressure drops by 0.1 bar. In all direct injection cases, by the end of the compression stroke, the mixture in the combustion chamber remains non-homogeneous, with leaner regions located near the intake valve.

- To achieve an equivalence ratio of $\varphi = 0.75$ at 250°CA, the injector opening angles are 80°CA, 50°CA, and 25°CA for engine speeds of 2000 rpm, 2400 rpm, and 2800 rpm, respectively. The corresponding residual cylinder pressures are 0.77 bar, 0.85 bar, and 0.89 bar; these represent increases of 100%, 97%, and 79%, respectively, compared to intake-based fueling systems.

- As engine speed increases, the evaporation duration of the pilot diesel spray becomes longer, yet it improves mixture uniformity. Under identical injection conditions, the difference between minimum and maximum fuel concentrations ranges from 13%–20% at 2000 rpm and narrows slightly to 14%–19% at 2800 rpm.

- Direct injection via a dual-injector system enhances the power output of dual-fuel engines, improves governor performance, and enables flexible use of gaseous renewable fuels such as syngas, biogas, and hydrogen, supporting compatibility with hybrid renewable energy systems.

- It is possible to fabricate an ECU to control the direct injection of flexible syngas-biogas-hydrogen fuel based on the simulation results in Proteus. The direct injection nozzle has an injector that opens in the opposite direction compared to the injector supplying fuel on the intake manifold.

Acknowledgments: The authors wish to express their appreciation to the Ministry of Education and Training Vietnam for supporting this research under the project B2024.DNA.12, entitled "Smart controller for engine fueled with flexible gaseous fuels in hybrid renewable energy system".

REFERENCES

[1] Vietnamnews, "Việt Nam strives to achieve 'net zero' by 2050, with international support: PM", *vietnamnews.vn,* November 02, 2021. [Online]. Available: https://vietnamnews.vn/environment/1071075/viet-nam-strives-to-achieve-net-zero-by-2050-with-international-support-pm.html [Accessed April 02, 2025].

[2] S. Guo, Q. Liu, Jie Sun, and H. Jin, "A review on the utilization of hybrid renewable energy", *Renewable and Sustainable Energy Reviews*, Vol. 91, pp. 1121–1147, 2018 https://doi.org/10.1016/j.rser.2018.04.105

[3] I. Eziyi and A. Krothapalli. "Sustainable Rural Development: Solar/Biomass Hybrid Renewable Energy System", *Energy Procedia*, Vol. 57, pp. 1492-1501, 2014. https://doi: 10.1016/j.egypro.2014.10.141

[4] K. Bär, S. Wagender, F. Solka, A. Saidi, and W. Zörner, "Flexibility Potential of Photovoltaic Power Plant and Biogas Plant Hybrid Systems in the Distribution Grid", *Chemical Engineering & Technology*, Vol. 43, Issue 8, pp. 1571-1577, 2020. https://doi.org/10.1002/ceat.202000025

[5] Y.S. Mohammed, M.W. Mustafa, and N. Bashir. "Hybrid renewable energy systems for off-grid electric power: Review of substantial issues", *Renewable and Sustainable Energy Reviews*, Vol. 35, pp. 527–539, 2014. http://dx.doi.org/10.1016/j.rser.2014.04.022,

[6] K.S. Krishna and K. S. Kumar, "A review on hybrid renewable energy systems", *Renew Sustain Energy Rev*, Vol. 52, pp. 907-916, 2015. https://doi.org/10.1016/j.rser.2015.07.187

[7] B. V. Ga, V. T. Hung, B. T. M. Tu, T. L. B. Tram, and N. T. T. Xuan, "Characteristics of Biogas-Hydrogen Engines in a Hybrid Renewable Energy System", *International Energy Journal*, Vol. 21, No. 4, pp. 467-480, 2021.

[8] B. V. Ga, V. A. Vu, H. V. Thanh, N. X. Thinh, N. T. Tin, and H. Q. Bao, "Design of a press for RDF production from household waste". *The University of Danang - Journal of Science and Technology*, Vol. 19, No. 2, pp. 13-17, 2021.

[9] B. V. Ga, B. T. M. Tu, H. C. Ong, Sandro Nižetić, B. V. Hung, N. T. T. Xuan, and A.E. Atabani, *et al.,* Optimizing operation parameters of a spark-ignition engine fueled with biogas-hydrogen blend integrated into biomass-solar hybrid renewable energy system, *Energy*, Vol. 252, 2022. https://doi.org/10.1016/j.energy.2022.124052

[10] T. V. Nam, B. V. Ga, P. M. Duc, and B. T. M. Tu, "Using biogas-hydrogen fuel for a spark-ignition engine driving a generator in a hybrid renewable energy system", in *Proceedings of the 21st National Conference on Fluid Mechanics and Hydraulics*, Quinhon, 2018, pp. 448-458.

[11] B. V. Ga, V. A. Vu, B. T. M. Tu, B. V. Hung, T. L. B. Tram, and P. V. Quang, "Air/fuel ratio control of an si-engine fueled with poor Biogas-HHO", *The University of Danang - Journal of Science and Technology*, Vol. 17, No. 3, 2019.

[12] T. L. B. Tram, B. V. Ga, N. T. T. Xuan, and P. V. Quang, "Simulation of Biogas-HHO flexible fuel supply for a si engine", in *Proceedings of the 22nd National Conference on Fluid Mechanics and Hydraulics*, Haiphong, 2019, pp. 772-783.

[13] B. V. Ga, T. V. Nam, H. A. Tuan, B. T. M. Tu, and V. A. Vu, "A simulation study on a port-injection SI engine fueled with hydroxy-enriched biogas", *Energy Sources, Part A: Recovery, Utilization, and Environmental Effects*, Vol. 46, Issue 1, pp. 13706-13722, 2020. https://doi.org/10.1080/15567036.2020.1804487

[14] B. V. Ga, B. T. M. Tu, T. L. B. Tram, N. D. Hoang, and P. V. Quang, "A concept of engine map for engine fueled with biogas-gasoline", *The University of Danang - Journal of Science and Technology*, Vol. 17, No. 9, pp. 33-39, 2019

[15] B. V. Ga, L. M. Tien, B. V. Tan, and V. N. Tung, "Simulation of the Engine Map for a Hybrid-Fueled Engine Using Biogas and Gasoline", in *Proceedings of the 22nd National Conference on Fluid Mechanics and Hydraulics*, Haiphong, 2019, pp. 250-259.

[16] B. V. Ga, B. T. M. Tu, T. L. B. Tram, and B. V. Hung, "Technique of Biogas-HHO Gas Supply for SI Engine", *International Journal of Engineering Research & Technology (IJERT)*, Vol. 8, Issue 05, pp. 669-674, 2019.

[17] B. T. M. Tu, B. V. Hung, and T. L. B. Tram, "Study on Biogas-HHO Injection Technology in the Intake Manifold of a Stationary Spark-Ignition Engine", in *Proceedings of the 23rd National Conference on Fluid Mechanics and Hydraulics*, 2020, pp. 636-647.

[18] B. V. Ga, T. T. H. Tung, L. M. Tien, B. T. M. Tu, D. V. Nghia, and T. N. T. Sang, "Performance and pollution emissions of a biogas-HHO port injection engine", *The University of Danang - Journal of Science and Technology*, Vol. 18, No. 1, pp. 43-48, 2020.

[19] F. Hagos, A. Aziz, and S. Sulaiman, "Trends of syngas as a fuel in internal combustion engines", *Advances in Mechanical Engineering*, pp. 1-10, 2014.

[20] B. V. Ga *et al.*, "Flexible syngas-biogas-hydrogen fueling spark-ignition engine behaviors with optimized fuel compositions and control parameters", *International Journal of Hydrogen Energy*, Vol. 48, Issue 18, pp. 6722-6737 2022. https://doi.org/10.1016/j.ijhydene.2022.09.133

[21] C. Rakopoulos and N. Michos, "Development and validation of a multi-zone combustion model for performance and nitric oxide formation in syngas fueled spark ignition engine", *Energy Conversion and Management*, Vol. 49, Issue 10, pp. 2904-2498, 2008.

[22] W. Keith. *Have wood will travel complete plans for the Keith gasifier*. 1st edn, 2013.

[23] B. V. Ga, B. T. M. Tu, N. V. Giao, T. V. Nam, T. L. B. Tram, and P. L. H. Phu, "Concept of twining injector system for spark-ignition engine fueled with syngas-biogas-hydrogen operating in solar-biomass hybrid energy system", *International Journal of Hydrogen Energy*, Vol. 48, Issue 18, pp 6871-6890, 2022. https://doi.org/10.1016/j.ijhydene.2022.11.076

[24] B. V. Ga, N. V. Dong, C. X. Tuan, and V. A. Vu, "Simulation of syngas-biogas-hydrogen flexible fuel supply for a stationary SI engine", *The University of Danang - Journal of Science and Technology*, Vol. 20, No. 9, 2022.